LETTER

Flexible Textile Direct-Current Generator Based on the Tribovoltaic Effect at Dynamic Metal-Semiconducting Polymer Interfaces

Jia Meng, Zi Hao Guo, Chongxiang Pan, Luyao Wang, Caiyun Chang, Longwei Li, Xiong Pu,* and Zhong Lin Wang*

Read Online

ACCESS | Metrics & More | Article Recommendations | Supporting Information

ABSTRACT: Generation of direct current (DC) from mechanical kinetic energies is crucial for realizing self-powered wearable electronics. Here, we report a flexible textile-based DC generator based on the tribovoltaic effect at a dynamic metal-semiconducting polymer interface. The tribovoltaic effect refers to a phenomenon in which an energy "quantum" is released once an atom−atom bond is formed at the dynamic interface of two contacting materials; such released "binding" energy excites electron−hole pairs at metal−semiconductor interfaces or semiconductor−semiconductor pn junctions. This textile DC generator, based on the dynamic Schottky junction between an Al slider and a poly(3,4-ethylenedioxythiophene)-coated textile, can output a voltage of approximately 0.45−0.70 V. The voltage and current can be increased by simply connecting multiple generators in series or in parallel. Seven generators in series can power an electronic watch constantly without any conditioning circuit. These findings offer an efficient strategy for harvesting mechanical energies and realizing self-powered electronics.

Flexible tribovoltaic DC generator
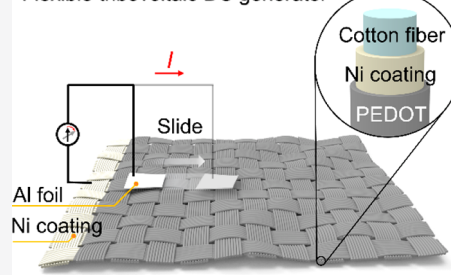
Kinetic energy harvesting is crucially important for the development of wearable electronics and the Internet of things.[1−5] The energy of a battery is always limited, especially considering the pursuit of lightweight and miniature electronics, while renewable kinetic energy is free, ubiquitous, and sustainable.[6,7] Therefore, developing a power-generating device to convert mechanical energies into electricity is essential to achieve self-powered electronics.[8,9] The advent of triboelectric nanogenerators (TENGs) can solve part of this problem, which generate electric energy from various types of mechanical motions (human motion, vibration, rotation, wind, raindrop, ocean waves, etc.) based on the coupling effect of contact electrification and electrostatic induction.[10−12] Conventional TENGs generally supply electricity in the form of alternating current with a high internal impedance; therefore, designing conditioning circuits for alternating-current (AC)−direct-current (DC) conversion and impedance matching is indispensable. In this case, the energy utilization efficiency is increased and the miniaturization and intelligent integration with functional sensors are difficult.[13] Therefore, flexible DC generators with low internal impedance are in high demand.

Several strategies have been reported to realize wearable devices that generate DC electricity from kinetic energy. First, DC electricity has been generated on the basis of the automatic switch of the two electrodes of a TENG with appropriate

mechanical designs, but the intrinsic mechanism is still the same as that of an AC TENG.[14] Another approach is based on the coupled effects of contact electrification and dielectric breakdown.[15] The dielectric breakdown at the gap between one electrode and the electrified film results in a direct-current loop between the two electrodes. These two approaches share the common characteristic that charge transfers at the dynamic interfaces lead to the generation of electrostatic charges in the surface of dielectric materials. Recently, a third discovery was reported to generate DC current from dynamic metal−insulator−semiconductor (MIS) interfaces,[16−18] dynamic P/N-type semiconductor interfaces,[19−21] or dynamic metal−semiconductor (MS) interfaces.[22−27] Specifically, friction motions are designed at the dynamic PN junctions, Schottky MS interfaces, or MIS interfaces to excite non-equilibrium charge carries, which are separated by the built-in field to output DC current to the external circuits. The static metal−
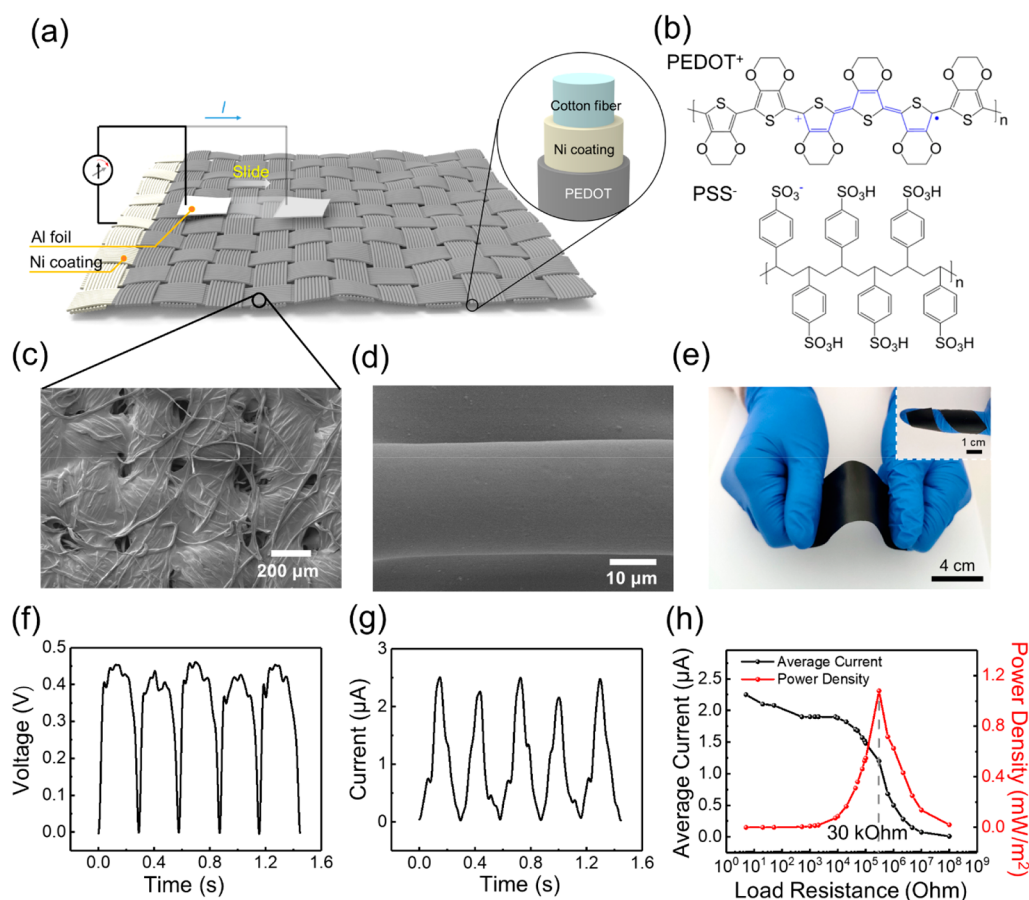
Figure 1. Structure and fabrication of the textile tribovoltaic DC generator. (a) 3D schematic diagram of a textile tribovoltaic DC generator, which consists of a PEDOT- and Ni-coated textile and an Al foil slider. (b) Molecular structure of PEDOT$^+$ and PSS$^-$. (c and d) SEM images of the textile and a single fiber, respectively, with PEDOT coatings. (e) Photograph of a PEDOT/Ni-coated textile. (f) Typical V_{oc} and (g) I_{sc} of a textile tribovoltaic DC generator with a slider area of 1 cm^2 and a pressure force of 0.15 N. (h) Variation of current and power density of the DC generator with the external load resistance.

semiconductor or semiconductor—semiconductor interfaces have been thoroughly studied and are the fundamentals of many electronic devices, whereas little about these dynamic interfaces has been explored until the recent reports. The detailed mechanism still requires further investigations, and there is still debate about the explanation of these phenomena. According to recent studies, we termed this mechanical-to-electrical energy conversion as the tribovoltaic effect, in which an energy "quantum" is released once an atom—atom bond is formed at the dynamic interface of two contacting materials, and such released "binding" energy would excite electron—hole pairs at a metal—semiconductor interface or semiconductor—semiconductor PN junctions, analogous to the photovoltaic effect.[28] The electrons are then separated from the holes due to the built-in electric field at the interface. The tribovoltaic effect occurs even in the contacting of a liquid and a semiconductor.[29] The DC generators based on the tribovoltaic effects feature the characteristics of a high current output and a low internal impedance, suggesting great promise for self-powered electronics. Nevertheless, flexible tribovoltaic DC generators with high output performances are still not demonstrated yet. Furthermore, the electricity generation mechanism and its practical viability need further to be investigated in depth, as well.

In this work, we achieved a flexible tribovoltaic DC generator at the metal-semiconducting polymer interfaces on

a textile substrate. Asymmetric MS contacts were achieved at the poly(3,4-ethylenedioxythiophene) (PEDOT), which was coated on a Ni-coated textile substrate. The energy released for forming an atom—atom bond at the dynamic Schottky contact between an Al slider and the PEDOT coating can be absorbed to excite non-equilibrium electron—hole pairs, which were separated by the built-in electric field. The accumulated potential energy difference at the interface then outputs voltage and electric work to the external circuit. A single DC generator based on this tribovoltaic effect can output a voltage of approximately 0.45−0.70 V and a current of approximately 2.5−10 μA. Excellent flexibility and durability were also demonstrated. Self-powered electronics were demonstrated using seven DC generators connected in series, which were able to power an electronic watch continuously. This flexible textile-based generator showed high DC outputs with a low internal impedance, leading to the efficient energy utilization when being directly connected to electronics without conditioning circuits. Therefore, our work suggested highly promising potentials for future applications in wearable electronics.

We proposed to construct tribovoltaic DC generators with dynamic metal—polymer semiconductor interfaces, considering potentially better flexibility of semiconducting polymers than inorganic semiconductors. Figure 1a shows a three-dimensional (3D) schematic diagram of the as-prepared flexible
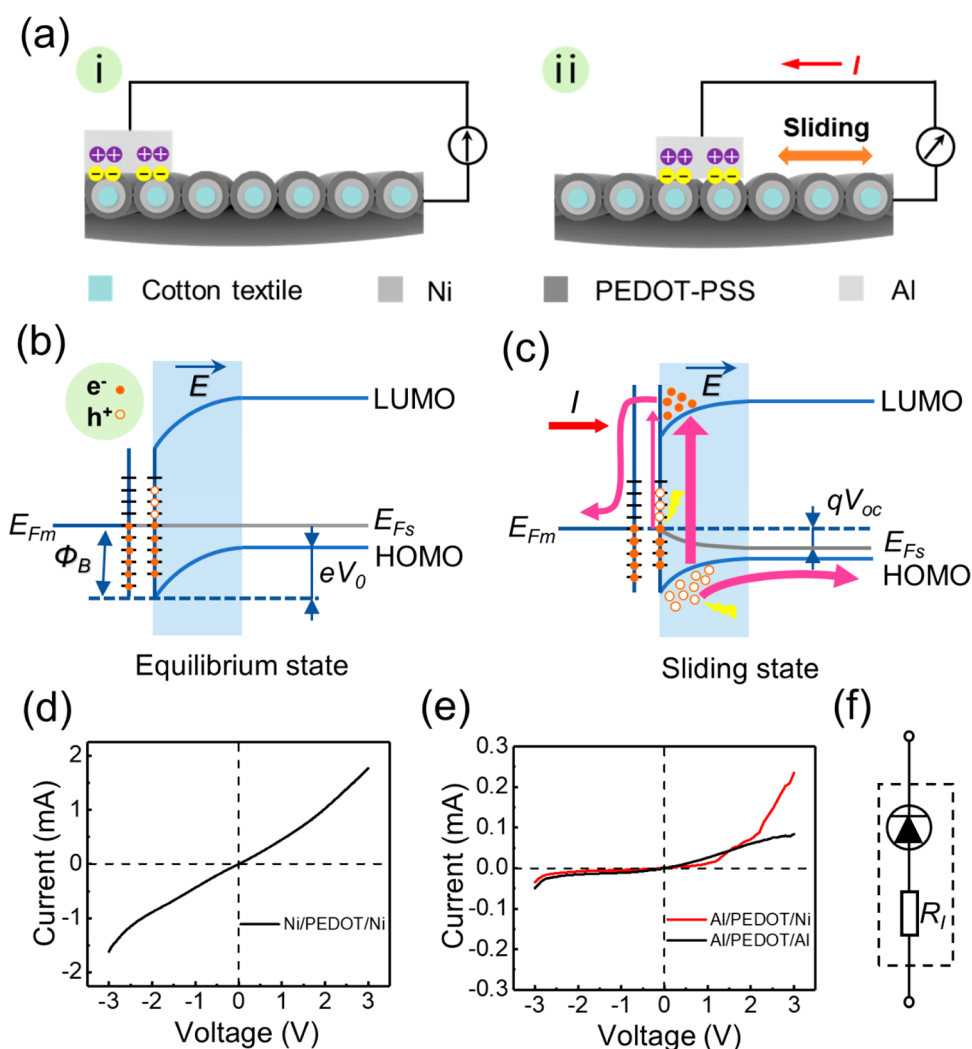
Figure 2. Working principle of the textile tribovoltaic DC generator. (a) Schematic illustration of the electricity generation process of the tribovoltaic DC generator. (b and c) Energy band diagram of the Al−PEDOT interface in the equilibrium state and sliding state, respectively. Current−voltage curves of the (d) Ni−PEDOT−Ni and (e) Al−PEDOT−Al and Al−PEDOT−Ni with a contact area of 4 cm^2 under a pressure of 5 N. (f) Equivalent circuit of the DC generator.

tribovoltaic DC generator. The polymer semiconductor, i.e., lightly doped PEDOT in this study, was coated on a conductive Ni-coated textile substrate. When sliding a thin Al foil on the PEDOT-coated textile, we found direct current will be generated flowing from the Ni coating layer to the Al foil. In this study, the PEDOT was lightly doped with poly(styrenesulfonate) (PSS) as depicted in Figure 1b, for the following considerations. First, the PEDOT-PSS remained semiconducting with holes as the dominating charge carriers at a low doping level. The PEDOT-PSS was used as received (J&K Scientific, 184174) without a secondary doping treatment (such as the treatment with DMSO). PEDOT chains can be doped to different degrees ranging from 0% to 33% of monomer units through oxidization by the counterions (i.e., PSS).[30,31] After the secondary doping treatment with DMSO, the PEDOT$^+$-PSS$^−$ can typically achieve conductivity close to 1000 S/cm and become metallic.[32] Nevertheless, if not being treated with DMSO, the PEDOT-PSS remains to be p-type semiconducting and its conductivity is typically <1 S/cm.[33] The conductivity of the as-received PEDOT-PSS was measured to be 0.02 S/cm, confirming that the PEDOT chains were almost still neutral. Second, the PSS helps the

uniform dispersion of the PEDOT in water and is beneficial for the formation of tight coating layers on the fiber substrates. The FTIR spectrum showed that the main characteristic peaks of PEDOT and PSS were found (Figure S1), evidencing the existence of PEDOT and PSS in the textile.[34,35] As shown in Figure 1c, the dip coating PEDOT layer covered the porous fabric substrate, but the large pores between warp and weft yarns remained. The porous morphology of the textile, in fact, helps to improve the binding between the PEDOT coating and the substrate, as well. The smooth and conformal PEDOT coating on a single fiber was also confirmed (Figure 1d). The PEDOT-coated textile could be bent (Figure 1d) and twisted around a finger (inset in Figure 1e), suggesting its excellent flexibility.

When sliding back and forth an Al foil (the area is 1 cm^2, and the pressure force is 0.15 N) on the PEDOT-coated textile, we found the representative open-circuit voltage (V_{oc}) profile and short-circuit current (I_{sc}) profile (panels f and g of Figure 1, respectively). Each sliding motion generated a DC electricity pulse. The amplitude of the V_{oc} and I_{sc} reached ∼0.45 V and ∼2.5 μA, respectively. Upon comparison with many reported AC TENGs, the voltage is several orders of
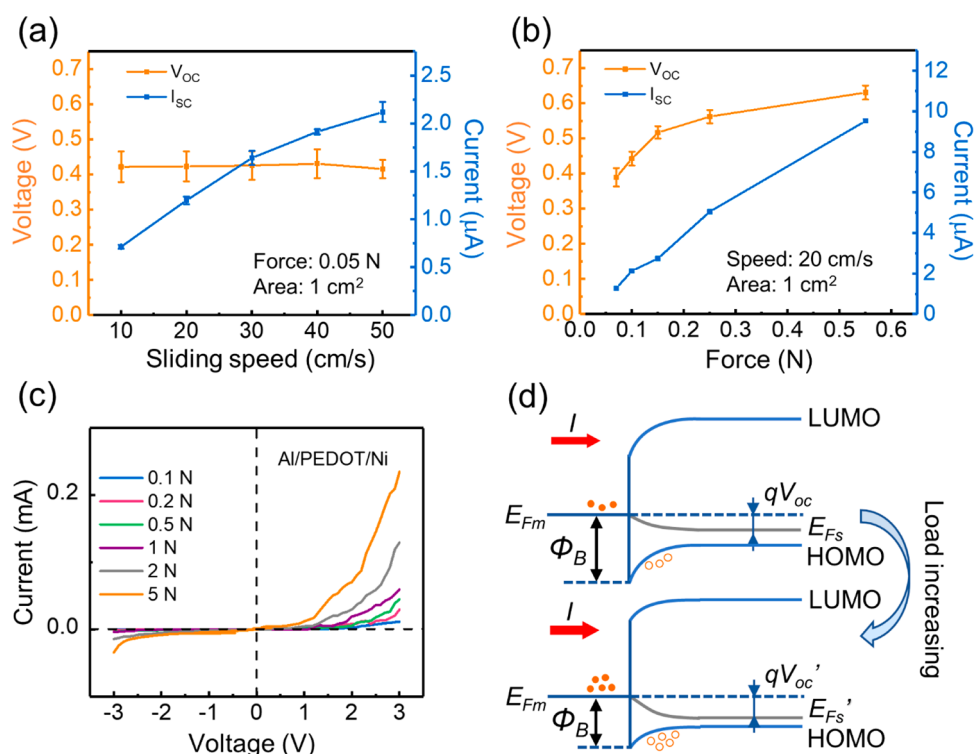
Figure 3. Influencing factors for the textile tribovoltaic DC generator. (a and b) Variation tendencies of V_{oc} and I_{sc} with different sliding speeds and pressure forces, respectively. (c) Current−voltage profiles of the Al−PEDOT−Ni system under different pressure forces. (d) Energy band diagram of the Al−PEDOT interface under low and high load pressures.

magnitude lower but the current is high.[36−38] Furthermore, the power density reached 1.1 mW/m² at a matching impedance of ∼30 kOhm (Figure 1h). Upon comparison with AC TENGs, the high current output and low internal impedance of the textile DC generator make it easier to integrate with self-powered electronics. Comprehensive comparisons with reported tribovoltaic DC generators are also shown in Table S1. The output of our flexible textile device is higher than or comparable with those of most tribovoltaic devices using inorganic semiconductors.

The work cycle and principle of the textile DC generator are schematically illustrated in Figure 2a. Metal Al and Ni have work functions of ∼4.28 and ∼5.15 eV, respectively.[39] The neutral PEDOT without doping has a band gap in the range of 1.5−1.7 eV.[31,40] The highest occupied molecular orbital (HOMO) and lowest unoccupied molecular orbital (LUMO) of neutral PEDOT are ∼3.9 and ∼5.4 eV, respectively.[41] With an increase in the doping level with PSS, the band gap will decrease and the work function will increase to ∼5.1 eV.[42] As stated above, the doping level of PEDOT in this study was very low and close to being neutral judging from the conductivity. We further measured the work function of the PEDOT in this study using ultraviolet photoelectron spectroscopy (UPS), which was determined to be 4.8 eV (Figure S2). Therefore, considering the hole as a dominating charge carrier in the PEDOT, it is safe to expect that ohmic contact will be formed at the Ni−PEDOT interface, while Schottky contact will be formed at the Al−PEDOT interface, as illustrated by the energy band diagram at the Al−PEDOT interface in Figure 2b. When the Al slider is in contact with a PEDOT-coated textile, the more energetic electrons in the Fermi level of the Al can readily diffuse into the PEDOT in search of lower empty energy levels. The diffusion of electrons

causes the PEDOT surface to be negatively charged while the Al surface to be positively charged, leading to the establishment of a built-in electric field (E) pointing from the positive charges to the negative charges in the thin space charge region at the PEDOT side. Eventually, equilibrium is achieved when diffusion of the electron from the Al to PEDOT is balanced by drifting motion of electrons from the PEDOT to Al driven by the built-in field. The Fermi level is then aligned, and energy bands of PEDOT bend downward in the space charge region. As long as the Al remains still, no current flows through the external circuit (Figure 2a, i). Nevertheless, when the Al is sliding on the PEDOT, non-equilibrium carriers can be generated in the space charge region by the friction energy at the interface. The energy dissipated by the relative friction motion can be absorbed by electrons, so that they can jump to the LUMO of the PEDOT and drift against the direction of built-in field; in the meantime, induced holes can drift along the built-in field (Figure 2c). On the contrary, the electrons on the Al and PEDOT surface state absorbed friction energy can jump to a higher energy level, which then has chances to tunnel through the interface and contributes to the moving carriers, as well. Due to the excitation of non-equilibrium carriers, the Fermi level of PEDOT will decline and a potential energy difference (qV_{oc}) between the Al and PEDOT is formed, which can then do electrical work to an external circuit. Therefore, current flows from the Ni electrode to the Al slider when there is relative sliding motion between the Al- and PEDOT-coated textile (Figure 2a, ii).

This tribovoltaic process is very similar to the photovoltaic process.[25,26,28] The difference is that the mechanical energy that dissipated in the sliding process contributes to the excitation of electron−hole pairs. The atom−atom interaction or bonding through the electron cloud overlap when two
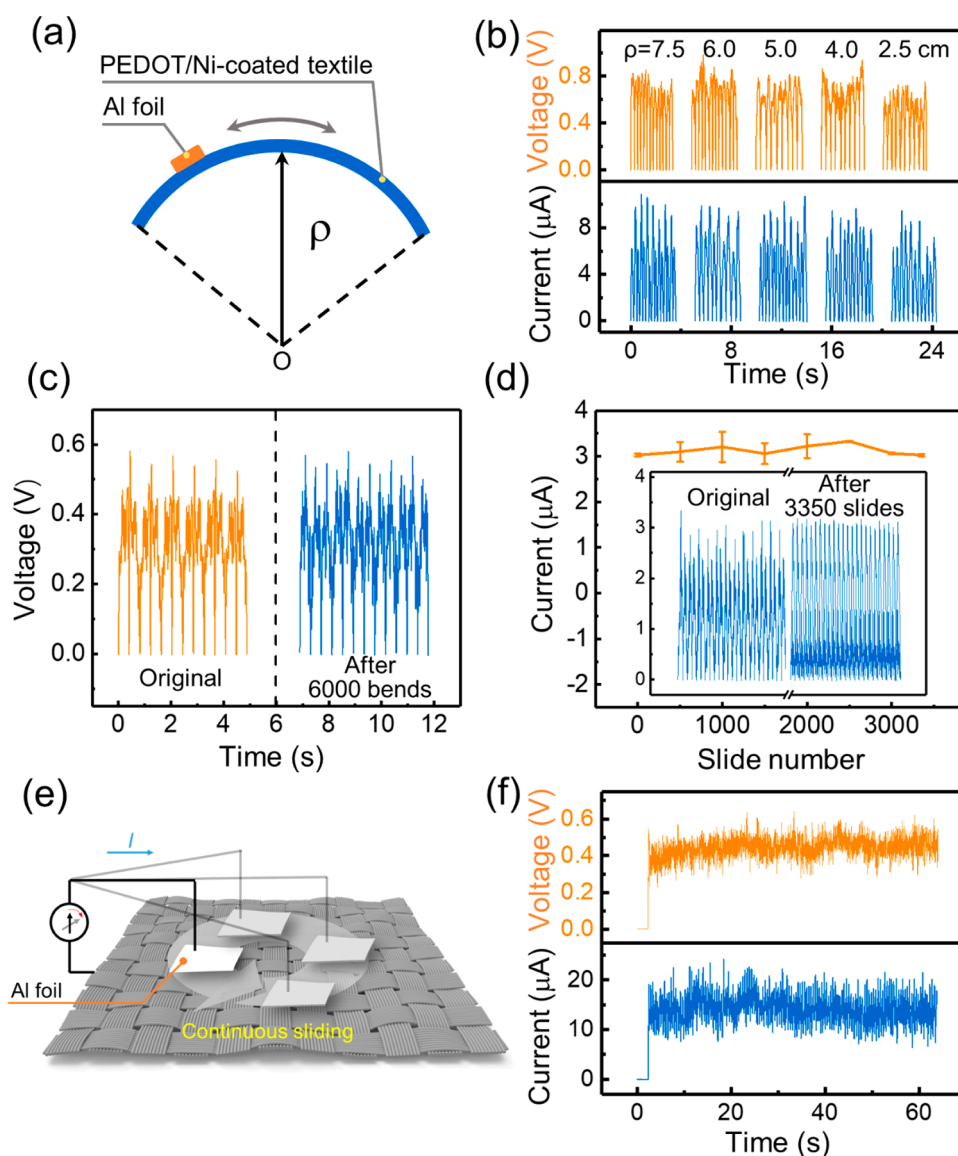
Figure 4. Flexibility and durability of the textile tribovoltaic DC generator. (a) Schematic diagram of the sliding of the Al foil on the curved textile. (b) V_{oc} and I_{sc} of the generator when sliding Al foil on the textile with different curvature radii. (c) V_{oc} of the tribovoltaic DC generator in the original state and after being bent 6000 times (1 cm curvature) under the linearly reciprocating mode with a 0.15 N pressure force and a slider area of 1 cm^2. (d) Long-term current output of the tribovoltaic generator with a slider area of 1 cm^2 and a pressure force of 0.15 N. (e) Schematic diagram of the tribovoltaic generator with an Al circular slider sliding continuously on the textile by a finger. (f) Continuous DC voltage and current outputs corresponding to panel e. The area of the textile used in the circular motion test is 10 cm × 10 cm.

surfaces are sufficiently close together has been demonstrated between many different materials.[43] Here, the atom−atom interactions at the interfaces are dynamically broken and formed during the sliding motions. In the rear area against the sliding direction, the atom−atom interactions in the depletion region are broken with the aid of the mechanical energies, while in the newly formed interface areas, new atom−atom interactions are formed, which release energy. In particular, the interaction with high-energy level dangling bonds possibly existing at the material surfaces can further add up to released energies. The released energy quantum would then generate electron−hole pairs at the interface. The built-in electric field is also crucial, which separates the electron−hole pairs and inhibits them from recombination. Therefore, the equivalent circuit diagram of the tribovoltaic DC generator is equivalent to a diode with an internal resistance R_I (Figure 2f).

According to the analysis presented above, asymmetric MS contacts with rectification characteristic are crucial for the tribovoltaic generators. Therefore, current−voltage profiles were measured by sandwiching the PEDOT-coated textile with Ni foils or Al foils. The Ni−PEDOT−Ni system showed a linear I−V characteristic (Figure 2d); the Ni−PEDOT−Al system showed a rectifying characteristic, while the Al−PEDOT−Al system exhibited a low current for both positive and reverse bias voltages (Figure 2e), confirming the formation of ohmic contact at the Ni−PEDOT interface and Schottky contact at the Al−PEDOT interface.

The parameters influencing the output performances of the textile tribovoltaic generator were then studied systematically, i.e., sliding speed and load pressure. The area of the Al slider was fixed to be 1 cm^2 for these tests. The load pressure was varied by putting different weights on top of the Al slider, while
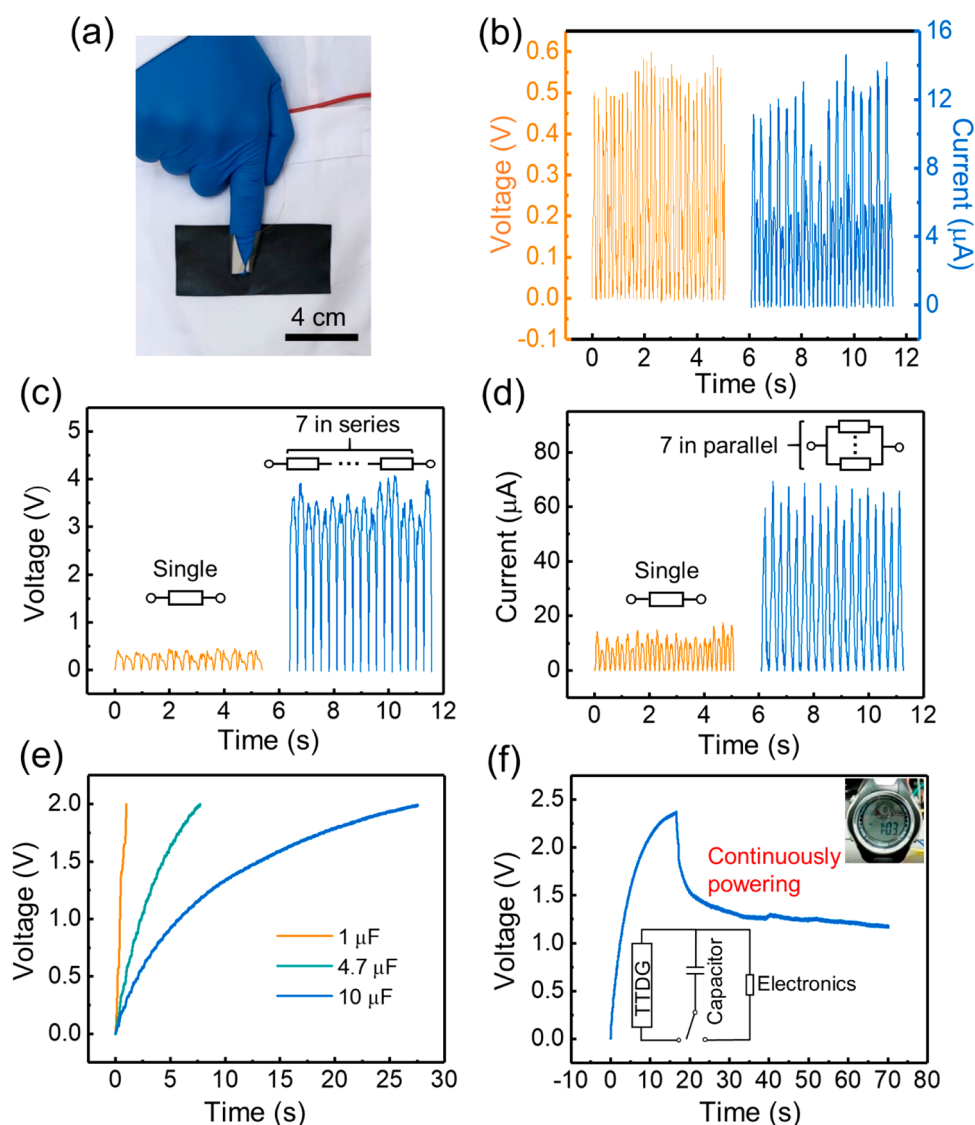
Figure 5. Application of a textile tribovoltaic DC generator (TTDG) in self-powered electronics. (a) Photo of a textile tribovoltaic generator integrated on a cloth. (b) V_{oc} and I_{sc} of a single tribovoltaic generator when sliding an Al-attached finger on the cloth. (c and d) V_{oc} and I_{sc} of seven devices connected in series and in parallel, respectively. (e) Voltage profiles of three capacitors charged by seven tribovoltaic generators connected in series. (f) A digital electronic watch (inset) was powered continuously by the seven tribovoltaic generators.

the sliding speed was controlled by a linear motor. When the load pressure is fixed to 0.05 N and the sliding velocity increases from 10 to 50 cm s^{-1}, the average I_{sc} increases from 0.75 to 2.2 μA, while the average V_{oc} maintains at about 0.40 V as shown in Figure 3a. Increasing the sliding speed means more dissipated friction energy, which then excites more electrons and holes at the MS interface and thereby increases the current. When the sliding speed is fixed at 20 cm s^{-1} and the load is increased from 0.05 to 0.55 N, the average I_{sc} of the generator increases significantly from 1.5 to 9.5 μA, while the V_{oc} increases gradually and reaches saturation around ∼0.62 V (Figure 3b). To explain this trend, the I−V curves of the Ni−PEDOT−Al system at different loading forces were measured (Figure 3c). The current density (J) of a Schottky contact interface at positive bias voltage can be written as

$$J = A^* T^2 \exp\left(-\frac{\Phi_B}{kT}\right)\left[\exp\left(\frac{eV}{kT}\right) - 1\right] \tag{1}$$

where A^* is the effective Richardson constant, k is the Boltzmann constant, T is the absolute temperature, V is the applied voltage, and Φ_B is the effective Schottky barrier potential. It is found that the current density under positive bias increases significantly with load force, which means that the effective barrier potential is decreased. Furthermore, the higher pressure also leads to more intimate contact at the interface and stronger friction energy. Therefore, more electron−hole pairs are generated and separated, contributing to a higher current. In the meantime, the Fermi level of the PEDOT decreases slightly toward the HOMO to a lower energy level, resulting in a gradual increase in V_{oc} (Figure 3d). We therefore conclude that the output current can be significantly improved by increasing the sliding speed or applied pressure during sliding, while the voltage tends to be insensitive to the sliding speed but varies slightly with pressure.

To demonstrate the flexibility of the textile tribovoltaic generator, the performances were measured when sliding the Al slider by hand on the PEDOT-coated textile attached to a

cylinder surface with different curvature radii, as shown in Figure 4a. When the curvature radius decreases from 7.5 to 2.5 cm, the output V_{oc} and I_{sc} are maintained at ~0.7 V and ~10 μA, respectively (Figure 4b), confirming that the generator operates appropriately in the bending states. The higher output voltage and current observed when sliding with hands were attributed to the possibly higher pressure and sliding speed than that using the linear motor. The textile was then bent to an ~1 cm curvature radius for 6000 cycles by a linear motor (Figure S3). No noticeable decrease in the outputs was observed, as shown in Figure 4c, demonstrating its excellent flexibility. The durability of the textile DC generator was evaluated by long-term measurement for 3350 cycles of back-and-forth sliding motions using the linear motor (1.25 Hz frequency and 0.15 N pressure force). The current output is basically stable throughout the testing period (Figure 4d). Furthermore, no significant damage on the surface morphology of the textile was observed in the original state and after 3350 cycles of sliding motions (Figure S4). We also tested the output before and after completely folding the PEDOT−Ni−fabric in half three times. One can see that the voltage output is basically stable while the current output is slightly decreased before and after folding (Figure S5a,b). The textile generator was foldable, but there were traces left after complete folding (Figure S5c). It should be pointed out that damage to the PEDOT coatings was observed after long-term sliding at a high loading force ($\gtrsim$1 h under ~1 N force).

The outputs mentioned above were all measured under back-and-forth sliding motions, which generated intermittent DC outputs. As depicted in Figure 4e, continuous DC outputs would be achieved if the sliding motion was continuous. Indeed, a continuous voltage of ~0.4 V and a continuous current of ~15 μA were obtained by hand rubbing the PEDOT-coated textile with the Al slider for >1 min, as shown in Figure 4f.

To further demonstrate the practical applicability of this textile DC generator, we measured its output performances when wearing it on the human body. As shown in Figure 5a, a piece of the textile generator was sewn on a lab coat, and an Al foil was attached on an index finger for rubbing the PEDOT-coated textile. The obtained V_{oc} was ~0.5 V, and the I_{sc} was ~12 μA (Figure 5b). What is more important is the fact that we demonstrated that the textile generators can be connected in series or in parallel to improve the voltage or current. Seven textile generators were fabricated, as shown by the photo in Figure S6. When seven generators were connected in series, the open-circuit voltage reached ~3.5 V (Figure 5c), while the short-circuit current reached ~70 μA when the seven generators were connected in parallel (Figure 5d). In particular, the voltage of the seven generators connected in series was sufficiently high for charging batteries, or directly powering many electronics. Therefore, the seven generators in series were connected to charge a series of capacitors. The 1 μF capacitor took only $\lesssim$1 s to reach 2 V, while it took ~10 and ~27 s for 4.7 and 10 μF capacitors to reach 2 V, respectively (Figure 5e). The 4.7 μF capacitor was first charged to ~2.3 V by the seven generators in series and then was used to power an electronic watch (Figure 5f). After the electronic watch was connected, the rubbing motion of the textile generator was not stopped. The electronic watch was continuously operating for ~1 min, during which the voltage of the capacitor ramained stable at approximately 1.2−1.5 V. This means that energy output by the generators and the

energy consumed by the electronic watch were almost balanced, and a self-powered electronic was demonstrated. This process was also recorded in Video S1. Upon comparison with conventional AC TENGs, it was confirmed that highly efficient energy utilization was achieved without rectifying or impedance conditioning circuits.

In conclusion, we realized DC electricity generation from mechanical sliding motions by a flexible PEDOT-coated textile with asymmetric MS interfaces. The dynamic Schottky interface was demonstrated to be able to absorb dissipated friction energies to generate non-equilibrium electron−hole pairs and output voltage to the external circuit. Such an effect is attributed to the tribovoltaic effect reported recently. We then demonstrated the flexibility and durability of the DC generator and further showed that the output can be simply amplified by connecting multiple devices in series or in parallel. Due to the DC characteristics and low internal impedance, self-powered wearable electronics were achieved without conditioning circuits. This work showed a first flexible and practically viable tribovoltaic DC generator, which holds great promise for the future applications in wearable electronics.

■ ASSOCIATED CONTENT

Ⓢ Supporting Information

The Supporting Information is available free of charge at https://pubs.acs.org/doi/10.1021/acsenergylett.1c00288.

> All descriptions of experimental sections, including detailed fabrication of the flexible tribovoltaic DC generator, measurement methods, characterization of PEDOT-PSS, a table of comparison of various DC-TENGs in principle, materials and output performances, and additional references (PDF)
>
> (MP4)

■ AUTHOR INFORMATION

Corresponding Authors

Xiong Pu − *Center on Nanoenergy Research, School of Chemistry and Chemical Engineering, School of Physical Science and Technology, Guangxi University, Nanning 530004, P. R. China; CAS Center for Excellence in Nanoscience, Beijing Key Laboratory of Micro-nano Energy and Sensor, Beijing Institute of Nanoenergy and Nanosystems, Chinese Academy of Sciences, Beijing 101400, P. R. China; School of Nanoscience and Technology, University of Chinese Academy of Sciences, Beijing 100049, P. R. China;* ⓞ orcid.org/0000-0002-1254-8503; Email: puxiong@binn.cas.cn

Zhong Lin Wang − *CAS Center for Excellence in Nanoscience, Beijing Key Laboratory of Micro-nano Energy and Sensor, Beijing Institute of Nanoenergy and Nanosystems, Chinese Academy of Sciences, Beijing 101400, P. R. China; School of Nanoscience and Technology, University of Chinese Academy of Sciences, Beijing 100049, P. R. China; School of Materials Science and Engineering, Georgia Institute of Technology, Atlanta, Georgia 30332-0245, United States;* Email: zlwang@gatech.edu

Authors

Jia Meng − *Center on Nanoenergy Research, School of Chemistry and Chemical Engineering, School of Physical Science and Technology, Guangxi University, Nanning 530004, P. R. China; CAS Center for Excellence in*

Nanoscience, Beijing Key Laboratory of Micro-nano Energy and Sensor, Beijing Institute of Nanoenergy and Nanosystems, Chinese Academy of Sciences, Beijing 101400, P. R. China

Zi Hao Guo − CAS Center for Excellence in Nanoscience, Beijing Key Laboratory of Micro-nano Energy and Sensor, Beijing Institute of Nanoenergy and Nanosystems, Chinese Academy of Sciences, Beijing 101400, P. R. China; School of Nanoscience and Technology, University of Chinese Academy of Sciences, Beijing 100049, P. R. China

Chongxiang Pan − Center on Nanoenergy Research, School of Chemistry and Chemical Engineering, School of Physical Science and Technology, Guangxi University, Nanning 530004, P. R. China; CAS Center for Excellence in Nanoscience, Beijing Key Laboratory of Micro-nano Energy and Sensor, Beijing Institute of Nanoenergy and Nanosystems, Chinese Academy of Sciences, Beijing 101400, P. R. China

Luyao Wang − Center on Nanoenergy Research, School of Chemistry and Chemical Engineering, School of Physical Science and Technology, Guangxi University, Nanning 530004, P. R. China; CAS Center for Excellence in Nanoscience, Beijing Key Laboratory of Micro-nano Energy and Sensor, Beijing Institute of Nanoenergy and Nanosystems, Chinese Academy of Sciences, Beijing 101400, P. R. China

Caiyun Chang − Center on Nanoenergy Research, School of Chemistry and Chemical Engineering, School of Physical Science and Technology, Guangxi University, Nanning 530004, P. R. China; CAS Center for Excellence in Nanoscience, Beijing Key Laboratory of Micro-nano Energy and Sensor, Beijing Institute of Nanoenergy and Nanosystems, Chinese Academy of Sciences, Beijing 101400, P. R. China

Longwei Li − CAS Center for Excellence in Nanoscience, Beijing Key Laboratory of Micro-nano Energy and Sensor, Beijing Institute of Nanoenergy and Nanosystems, Chinese Academy of Sciences, Beijing 101400, P. R. China; School of Nanoscience and Technology, University of Chinese Academy of Sciences, Beijing 100049, P. R. China

Complete contact information is available at:
https://pubs.acs.org/10.1021/acsenergylett.1c00288

Author Contributions

X.P., Z.L.W., and J.M. conceived the project and designed the experiments. J.M. and C.P. contributed to sample preparation. J.M. and Z.H.G. performed the experiments. L.W., C.C., and L.L. contributed to data analysis. All authors discussed the results and commented on the manuscript. J.M., X.P., and Z.L.W. wrote the paper with input from all authors.

Notes

The authors declare no competing financial interest.

■ REFERENCES

(1) Gubbi, J.; Buyya, R.; Marusic, S.; Palaniswami, M. Internet of Things (IoT): A vision, architectural elements, and future directions. *Future Generation Computer Systems* **2013**, *29* (7), 1645−1660.

(2) Wang, Z. L.; Wu, W. Nanotechnology-enabled energy harvesting for self-powered micro-/nanosystems. *Angew. Chem., Int. Ed.* **2012**, *51* (47), 11700−11721.

(3) Zhu, J.; Liu, X.; Shi, Q.; He, T.; Sun, Z.; Guo, X.; Liu, W.; Sulaiman, O. B.; Dong, B.; Lee, C. Development Trends and Perspectives of Future Sensors and MEMS/NEMS. *Micromachines (Basel)* **2020**, *11* (1), 7.

(4) Zou, Y. J.; Raveendran, V.; Chen, J. Wearable triboelectric nanogenerators for biomechanical energy harvesting. *Nano Energy* **2020**, *77*, 105303.

(5) Chen, G. R.; Li, Y. Z.; Bick, M.; Chen, J. Smart Textiles for Electricity Generation. *Chem. Rev.* **2020**, *120* (8), 3668−3720.

(6) Fan, F. R.; Tang, W.; Wang, Z. L. Flexible Nanogenerators for Energy Harvesting and Self-Powered Electronics. *Adv. Mater.* **2016**, *28* (22), 4283−305.

(7) Xiao, G.; He, J.; Qiao, Y.; Wang, F.; Xia, Q.; Wang, X.; Yu, L.; Lu, Z.; Li, C.-M. Facile and Low-Cost Fabrication of a Thread/Paper-Based Wearable System for Simultaneous Detection of Lactate and pH in Human Sweat. *Adv. Fiber Mater.* **2020**, *2* (5), 265−278.

(8) Wang, S.; Lin, L.; Wang, Z. L. Triboelectric nanogenerators as self-powered active sensors. *Nano Energy* **2015**, *11*, 436−462.

(9) Pu, X.; Li, L.; Liu, M.; Jiang, C.; Du, C.; Zhao, Z.; Hu, W.; Wang, Z. L. Wearable Self-Charging Power Textile Based on Flexible Yarn Supercapacitors and Fabric Nanogenerators. *Adv. Mater.* **2016**, *28* (1), 98−105.

(10) Wang, Z. L. Triboelectric Nanogenerators as New Energy Technology for Self-Powered Systems and as Active Mechanical and Chemical Sensors. *ACS Nano* **2013**, *7* (11), 9533−9557.

(11) Pu, X.; Li, L.; Song, H.; Du, C.; Zhao, Z.; Jiang, C.; Cao, G.; Hu, W.; Wang, Z. L. A Self-Charging Power Unit by Integration of a Textile Triboelectric Nanogenerator and a Flexible Lithium-Ion Battery for Wearable Electronics. *Adv. Mater.* **2015**, *27* (15), 2472−2478.

(12) Zou, Y.; Libanori, A.; Xu, J.; Nashalian, A.; Chen, J. Triboelectric Nanogenerator Enabled Smart Shoes for Wearable Electricity Generation. *Research* **2020**, *2020*, 7158953.

(13) Shi, Q.; Sun, J.; Hou, C.; Li, Y.; Zhang, Q.; Wang, H. Advanced Functional Fiber and Smart Textile. *Adv. Fiber Mater.* **2019**, *1* (1), 3−31.

(14) Zhang, C.; Zhou, T.; Tang, W.; Han, C.; Zhang, L.; Wang, Z. L. Rotating-Disk-Based Direct-Current Triboelectric Nanogenerator. *Adv. Energy Mater.* **2014**, *4* (9), 1301798.

(15) Yang, Y.; Zhang, H.; Wang, Z. L. Direct-Current Triboelectric Generator. *Adv. Funct. Mater.* **2014**, *24* (24), 3745−3750.

(16) Liu, J.; Miao, M.; Jiang, K.; Khan, F.; Goswami, A.; McGee, R.; Li, Z.; Nguyen, L.; Hu, Z.; Lee, J.; Cadien, K.; Thundat, T. Sustained electron tunneling at unbiased metal-insulator-semiconductor triboelectric contacts. *Nano Energy* **2018**, *48*, 320−326.

(17) Liu, J.; Cheikh, M. I.; Bao, R.; Peng, H.; Liu, F.; Li, Z.; Jiang, K.; Chen, J.; Thundat, T. Tribo-Tunneling DC Generator with Carbon Aerogel/Silicon Multi-Nanocontacts. *Adv. Electron. Mater.* **2019**, *5* (12), 1900464.

(18) Liu, J.; Jiang, K.; Nguyen, L.; Li, Z.; Thundat, T. Interfacial friction-induced electronic excitation mechanism for tribo-tunneling current generation. *Mater. Horiz.* **2019**, *6* (5), 1020−1026.

(19) Xu, R.; Zhang, Q.; Wang, J. Y.; Liu, D.; Wang, J.; Wang, Z. L. Direct current triboelectric cell by sliding an n-type semiconductor on a p-type semiconductor. *Nano Energy* **2019**, *66*, 104185.

(20) Zhang, Q.; Xu, R.; Cai, W. Pumping electrons from chemical potential difference. *Nano Energy* **2018**, *51*, 698−703.

(21) Lu, Y.; Hao, Z.; Feng, S.; Shen, R.; Yan, Y.; Lin, S. Direct-Current Generator Based on Dynamic PN Junctions with the Designed Voltage Output. *iScience* **2019**, *22*, 58−69.

(22) Liu, J.; Goswami, A.; Jiang, K.; Khan, F.; Kim, S.; McGee, R.; Li, Z.; Hu, Z.; Lee, J.; Thundat, T. Direct-current triboelectricity generation by a sliding Schottky nanocontact on MoS2 multilayers. *Nat. Nanotechnol.* **2018**, *13* (2), 112−116.

(23) Lin, S.; Lu, Y.; Feng, S.; Hao, Z.; Yan, Y. A High Current Density Direct-Current Generator Based on a Moving van der Waals Schottky Diode. *Adv. Mater.* **2019**, *31* (7), 1804398.

(24) Lin, S.; Shen, R.; Yao, T.; Lu, Y.; Feng, S.; Hao, Z.; Zheng, H.; Yan, Y.; Li, E. Surface States Enhanced Dynamic Schottky Diode

Generator with Extremely High Power Density Over 1000 W m^{-2}. *Adv. Sci.* **2019**, *6* (24), 1901925.

(25) Zhang, Z.; Jiang, D.; Zhao, J.; Liu, G.; Bu, T.; Zhang, C.; Wang, Z. L. Tribovoltaic Effect on Metal−Semiconductor Interface for Direct-Current Low-Impedance Triboelectric Nanogenerators. *Adv. Energy Mater.* **2020**, *10* (9), 1903713.

(26) Zhang, Z.; He, T.; Zhao, J.; Liu, G.; Wang, Z. L.; Zhang, C. Tribo-thermoelectric and tribovoltaic coupling effect at metal-semiconductor interface. *Mater. Today Phys.* **2021**, *16*, 100295.

(27) Zheng, M.; Lin, S.; Xu, L.; Zhu, L.; Wang, Z. L. Scanning Probing of the Tribovoltaic Effect at the Sliding Interface of Two Semiconductors. *Adv. Mater.* **2020**, *32* (21), 2000928.

(28) Wang, Z. L.; Wang, A. C. On the origin of contact-electrification. *Mater. Today* **2019**, *30*, 34−51.

(29) Lin, S.; Chen, X.; Wang, Z. L. The tribovoltaic effect and electron transfer at a liquid-semiconductor interface. *Nano Energy* **2020**, *76*, 105070.

(30) Jönsson, S. K. M.; Birgerson, J.; Crispin, X.; Greczynski, G.; Osikowicz, W.; Denier van der Gon, A. W.; Salaneck, W. R.; Fahlman, M. The effects of solvents on the morphology and sheet resistance in poly(3,4-ethylenedioxythiophene)−polystyrenesulfonic acid (PEDOT−PSS) films. *Synth. Met.* **2003**, *139* (1), 1−10.

(31) Alcácer, L. Case study: PEDOT:PSS. In *Electronic Structure of Organic Semiconductors: Polymers and small molecules*; Morgan & Claypool: San Rafael, CA, 2018.

(32) Bubnova, O.; Khan, Z. U.; Wang, H.; Braun, S.; Evans, D. R.; Fabretto, M.; Hojati-Talemi, P.; Dagnelund, D.; Arlin, J. B.; Geerts, Y. H.; Desbief, S.; Breiby, D. W.; Andreasen, J. W.; Lazzaroni, R.; Chen, W. M.; Zozoulenko, I.; Fahlman, M.; Murphy, P. J.; Berggren, M.; Crispin, X. Semi-metallic polymers. *Nat. Mater.* **2014**, *13* (2), 190−194.

(33) Reynolds, J. R.; Thompson, B. C.; Skotheim, T. A. *Conjugated Polymers Properties, Processing, and Applications*; CRC Press: Boca Raton, FL, 2019.

(34) Kvarnström, C.; Neugebauer, H.; Blomquist, S.; Ahonen, H. J.; Kankare, J.; Ivaska, A. In situ spectroelectrochemical characterization of poly(3,4-ethylenedioxythiophene). *Electrochim. Acta* **1999**, *44* (16), 2739−2750.

(35) Seo, K. I.; Chung, I. J. Reaction analysis of 3,4-ethyl-enedioxythiophene with potassium persulfate in aqueous solution by using a calorimeter. *Polymer* **2000**, *41* (12), 4491−4499.

(36) Ye, C.; Xu, Q.; Ren, J.; Ling, S. Violin String Inspired Core-Sheath Silk/Steel Yarns for Wearable Triboelectric Nanogenerator Applications. *Adv. Fiber Mater.* **2020**, *2* (1), 24−33.

(37) Dong, S. S.; Xu, F.; Sheng, Y. L.; Guo, Z. H.; Pu, X.; Liu, Y. P. Seamlessly knitted stretchable comfortable textile triboelectric nano-generators for E-textile power sources. *Nano Energy* **2020**, *78*, 105327.

(38) Shuai, L.; Guo, Z. H.; Zhang, P.; Wan, J.; Pu, X.; Wang, Z. L. Stretchable, self-healing, conductive hydrogel fibers for strain sensing and triboelectric energy-harvesting smart textiles. *Nano Energy* **2020**, *78*, 105389.

(39) Neamen, D. A. *Semiconductor physics and devices basic principles*; McGraw-Hill: New York, 2012.

(40) Xing, K. Z.; Fahlman, M.; Chen, X. W.; Inganäs, O.; Salaneck, W. R. The electronic structure of poly(3,4-ethylene-dioxythiophene): studied by XPS and UPS. *Synth. Met.* **1997**, *89* (3), 161−165.

(41) Möller, S.; Perlov, C.; Jackson, W.; Taussig, C.; Forrest, S. R. A polymer/semiconductor write-once read-many-times memory. *Nature* **2003**, *426* (6963), 166−169.

(42) Koch, N.; Vollmer, A.; Elschner, A. Influence of water on the work function of conducting poly(3,4-ethylenedioxythiophene)/poly(styrenesulfonate). *Appl. Phys. Lett.* **2007**, *90* (4), 043512.

(43) Xu, C.; Zi, Y.; Wang, A. C.; Zou, H.; Dai, Y.; He, X.; Wang, P.; Wang, Y.-C.; Feng, P.; Li, D.; Wang, Z. L. On the Electron-Transfer Mechanism in the Contact-Electrification Effect. *Adv. Mater.* **2018**, *30* (15), 1706790.